

A microstrip patch-based antenna design using open circuit matching and slot-loading techniques for Wi-Fi / Bluetooth applications

M. D. Çalışır^{1,*}, H. S. Altaş¹, C. Murat¹

¹ Department of Electrical and Electronic Engineering, Recep Tayyip Erdogan University, Rize, Türkiye

ARTICLE INFO

Article Type:

Research Paper

Article History:

Received: 20 February 2025

Revised: 25 April 2025

Accepted: 5 May 2025

Published: 31 May 2025

Editor of the Article:

M. E. Şahin

Keywords:

Microstrip patch antenna, ISM band,
Open circuit matching, Slot-loaded
antenna

ABSTRACT

Microstrip patch antennas (MPAs) are widely used in various applications due to their compact structure, low cost, ease of fabrication, and wide bandwidth spectrum characteristics. In this study, impedance matching techniques are employed to design a directional antenna that operates within the Wi-Fi and Bluetooth bands, effectively utilizing the MPA spectrum. To enhance radiation performance, slot opening, and open circuit matching methods are applied to the conventional rectangular MPA structure. The designed antennas are simulated using finite element methods in the high-frequency structural simulator (HFSS) program and compared with actual antenna measurements. The experimental results show that the slotting and feed line stub insertion methods improve the antenna directivity by reducing the 3 dB beamwidth of the MPA by 10%. The proposed antenna exhibits an operational bandwidth ranging from 2.42 to 2.5 GHz with a return loss below -10 dB, effectively covering the 2.4 GHz Wi-Fi and Bluetooth frequency bands. Both simulation and measurement results show that the return loss, surface current distribution, and electric field distribution of the antenna meet the expected values. The design proves effective in wireless communication applications with a gain of 5.41 dBi.

Cite this article: M. D. Çalışır, H. S. Altaş, C. Murat, "A microstrip patch-based antenna design using open circuit matching and slot-loading techniques for Wi-Fi / Bluetooth applications," *Turkish Journal of Electromechanics & Energy*, 10(1), pp.3-9, 2025.

1. INTRODUCTION

Antenna designs are essential for high-speed and reliable wireless data transmission, and the performance of antennas in terms of directivity needs to be improved. Some of the directional antenna types used for this purpose are parabolic, horn, reflector, and Yagi-Uda antennas. Microstrip patch antenna (MPA) is also one of the directional antennas which consists of a radiating layer (patch) embedded in a dielectric substrate in the ground plane. The compact structure, low cost, and ease of fabrication of MPAs have enabled them to be widely used in wireless communications in recent years [1]. Television, radio, mobile phones, global positioning system (GPS), radio frequency identification (RFID), satellite systems, surveillance, radars, medical imaging, and missile guidance are just a few examples of military, civil, and industrial applications of MPAs [2, 3]. The 2.4 GHz industrial, scientific and medical (ISM) band used by Wi-Fi and Bluetooth faces significant interference due to numerous devices operating concurrently, which negatively impact signal quality, especially in long-distance communication scenarios. To mitigate interference and enhance signal strength in the intended direction, the antenna proposed in this study is designed as a directional antenna. Thus, higher gain and improved reliability are achieved for long-range wireless communication.

While microstrip patch antennas (MPAs) can be produced with simple geometries such as circular, triangular, square,

rectangular, etc., MPAs present disadvantages such as low bandwidth and gain [4]. To increase the bandwidth and gain, there are approaches such as using different radiation patterns in the radiating layer and/or in the ground plane and creating slots [5]. Erbaş [6] analyzed the performance of a dual-band (GSM-1800 and GPS) antenna designed with six rectangular slots in the ground plane. According to the simulation results, the resonant frequency (f_r) of the antenna without slots was 2.5 GHz, which decreased to 1.88 GHz with the slot implementation, rendering it suitable for the GSM-1800 band. In addition, the proportional bandwidths of the proposed antenna at -10 dB return loss were reported as 33.510% (1.540-2.160 GHz) and 15.130% (1.100-1.280 GHz) for GSM-1800 and GPS frequency bands, respectively. Chen et al. [7] presented a compact dual-band antenna design consisting of a rectangular slot, inverted-L-shaped and fork-shaped strips, and a defective ground plane. The slots and feed line facilitated favourable f_r at the lower band, while the fork-shaped and inverted-L patterns enabled resonance tuning for the high band. This design provided acceptable bandwidth for time division duplexing-long term evolution (TD-LTE) and WLAN 802.11 a/b/g applications.

Antenna impedance is a critical parameter that influences bandwidth and radiated power. Antenna impedance is a function of frequency, antenna geometry, physical dimensions, and feeding mechanism, with the operating frequency range

*Corresponding author's e-mail: mehmetdurmus.calisir@erdogan.edu.tr

determined by the impedance deviation from the standard 50 Ω . In practical designs, impedance mismatch significantly limits the achievable bandwidth [2]. However, antenna performance can be enhanced by achieving impedance matching using methods such as open circuit matching in the feed line. The primary advantage of impedance matching is that it increases the bandwidth and achieves the desired f_r without altering the patch geometry. By introducing a rectangular pattern of length l at a distance d from the patch, a capacitive or inductive loading effect is added to the feed line, as shown in Figure 1(a) [8].

In the circuit shown in Figure 1(b), the open-circuited shunt stub introduces a reactive susceptance B , which is placed in parallel with the transmission line. Here, B denotes the stub's susceptance in Siemens (S), representing its ability to conduct reactive current. In this study, the expression $t = \tan(\beta d)$ defines a coefficient that represents the phase shift along the transmission line, which depends on the phase constant β and the distance d . When the distance d and the stub length l are appropriately chosen, this susceptance cancels out the reactive component of the antenna admittance Y_L , resulting in a purely real input admittance that can be matched to 50 ohms. Consequently, the parameters l and d are determined according to Equation (1) and Equation (2) [9]. Figure 1(c) presents the lumped-element equivalent circuit of the proposed antenna. The model includes resistive (R_1), inductive (L), conductive (G), and capacitive (C_1 , C_2) components to represent feed line effects, dielectric losses, and open stub matching behaviour. The R_2 - C_2 branch models the impact of the open-circuited stub on impedance matching. This simplified circuit helps to interpret the antenna's electrical behaviour and guides the matching design analytically.

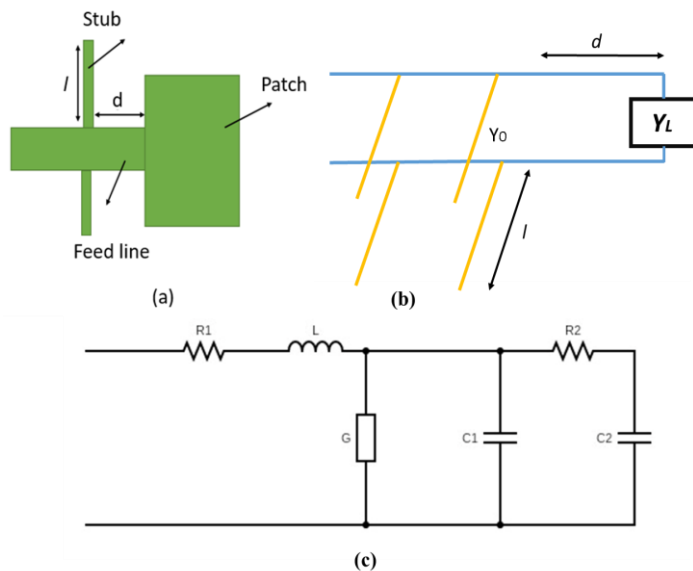


Fig. 1. (a) Patch antenna with stub structure, (b) The equivalent circuit of the stub in the patch antenna and (c) Lumped-element equivalent circuit of the antenna including RLC components and matching elements.

$$\frac{l}{\lambda} = \frac{1}{2\pi} \tan^{-1} \left(\frac{B}{Y_0} \right) \quad (1)$$

$$\frac{d}{\lambda} = \begin{cases} \frac{1}{2\pi} \tan^{-1}(t), & t \geq 0 \\ \frac{1}{2\pi} (\tan^{-1} t + \pi), & t < 0 \end{cases} \quad (2)$$

Sharma and Rishi [8] discussed various impedance-matching techniques and equations for MPA and calculated the input impedance of rectangular, circular, and triangular MPAs based on their techniques. Arai et al. [10] fabricated an impedance-matched, dual-frequency, dual-frequency, triple-stub patch antenna for mobile communication without utilizing active circuitry. Chen et al. [11] proposed a design for a polarization-sensitive microstrip line co-fed patch antenna. This antenna has a simple structure consisting of a square patch symmetrically loaded with two PIN diodes and a short-circuited stub. By using proximity-coupled feeding, natural impedance matching, along with radio frequency (RF) and DC signal isolation, is achieved without requiring DC-blocking components. The simulated antenna exhibits a gain of 2.77 dBi at 1.695 GHz and an efficiency of 43%. Mohan et al. [12] designed a matching circuit based on a stub-loaded transmission line for a Dolph-Tschebyshev amplitude-tapered series-fed patch array antenna. The f_r of the antenna was 78.75 GHz, with a gain of 9.27 dBi at this frequency.

In this study, unlike the existing MPA designs in literature, both open-circuit matching and patch pattern slotting modifications are applied simultaneously. Patch pattern slotting is also employed to fine-tune the f_r . The design targets covering the Wi-Fi/Bluetooth band (2.45 GHz) and achieving a return loss (S_{11}) below -10 dB. The proposed approaches are compared with conventional patch designs, and the antenna performances are evaluated.

2. EXPERIMENTAL RESULTS

Figure 2(a) and Figure 2(c) present the conventional MPA design without and with a stub, respectively, while Figure 2(b) and Figure 2(d) display the optimized antenna designs with slots and without/with stubs, respectively. The proposed patch antenna designs in Figure 2(a-d) were modelled using the finite element method (FEM) in ANSYS software high-frequency structural simulator (HFSS). The localized generation of electromagnetic radiation was examined using electric field and surface current analyses. An FR-4 epoxy substrate ($\epsilon_r = 4.4$) with dimensions of 50 \times 50 mm and a thickness of 3.2 mm was selected as the substrate material for the preparation of the optimised antenna design. Figure 2(e) and Figure 2(f) illustrate the antenna printed on a printed circuit board (PCB).

The structure of a rectangular patch antenna, one of the most fundamental forms of directional antennas, is shown in Figure 2(a). It features a grounded backside, which reflects radiation transmitted in that direction to the front side. To enhance the radiation efficiency of this rectangular patch antenna, specific modifications have been applied to the patch area. These modifications involve creating slits on the patch to disrupt the surface current, as illustrated in Figure 2(b). However, these modifications alter the conventional mathematical model of the patch antenna, causing its operating frequency to deviate from the original design target.

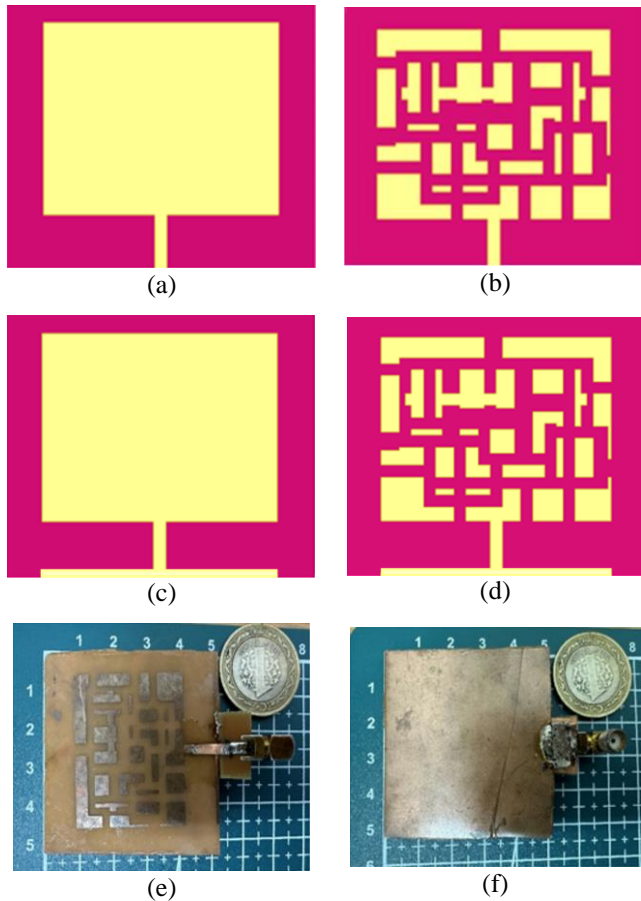


Fig. 2. (a) Conventional MPA design, (b) MPA with a slot but without a stub, (c) MPA with a stub but without a slot, (d) MPA with both a stub and a slot, and (e, f) Proposed realized MPA designs.

The stub structure applied in Figure 2(c) also allows for impedance tuning but does not contribute to radiation efficiency, as no modifications have been made to the patch itself. In contrast, as depicted in Figure 2(d), an open-circuit stub incorporated into the transmission line feeding the antenna provides a reactive contribution to the antenna impedance, enabling impedance matching at the desired frequency. The realized version of the proposed antenna design in Figure 2(d), is fabricated and presented in Figure 2(e) and Figure 2(f). The schematic representation of this design, along with the relevant design parameters, is provided in Figure 3, and the corresponding parameter values are listed in Table 1.

Antenna measurements were performed at the Recep Tayyip Erdoğan University Electromagnetic Application and Research Centre (REMAM). The S_{11} parameter was measured using an HP 8720A Vector Network Analyzer. The radiation pattern was recorded at 30° intervals in the x-y plane using the isotropic antenna of the NARDA SRM-3006 spectrum analyzer 9 kHz–6 GHz measurement bandwidth [13].



Fig. 3. Design of the proposed patch antenna.

Table 1. Dimensions (Dim.) of the proposed antenna.

Dim	Value (mm)	Dim	Value (mm)	Dim	Value (mm)
L1	6.55	L12	7.36	W1	17
L2	9.5	L13	7.36	W2	18
L3	11	L14	6.5	W3	3
L4	4	L15	8.64	W4	3
L5	4	L16	1	W5	5
L6	9.5	L17	2	W6	12
L7	8	L18	2.5	W7	5
L8	7	L19	4	W8	6
L9	7.36	L20	1	W9	18
L10	5	L21	50	W10	3
L11	5.36	L22	30.72	W11	50

3. MEASUREMENT RESULTS

According to Faraday's Law from Maxwell's equations, a time-varying current density generates a magnetic field, while Ampère's Law states that a time-varying magnetic field induces an electric field. This continuous interaction between the electric and magnetic fields results in the formation of electromagnetic radiation [2]. To achieve high performance at $f_r = 2.4$ GHz, the slot configuration was optimized based on electromagnetic theory. In particular, principles derived from Maxwell's equations played a crucial role in determining the geometry and layout of the slots. Additionally, an iterative optimization method was employed to fine-tune the position and dimensions of the slots, ensuring optimal performance based on simulation evaluations.

Iterative optimization is a widely used approach in antenna design, especially when analytical models become insufficient due to structural complexities such as slots and stubs. It involves systematically adjusting key design parameters (e.g., slot dimensions, stub positions, feed point location) and performing multiple simulations to evaluate their impact on critical performance metrics – including return loss, gain, and bandwidth. This trial-and-error process allows designers to fine-tune the geometry step by step, ensuring that the final configuration achieves optimal performance within the desired frequency band.

In this study, iterative optimization was applied to determine the most effective slot length and placement, which significantly

influenced impedance matching and radiation behaviour. A parameter analysis was conducted using the iterative optimization method. The slot length defined as w_2 was swept from 15 mm to 21 mm with 1 mm intervals, and the S_{11} performance was evaluated for each value. As shown in Figure 4, the best return loss (approximately -16 dB) was achieved at $w_2 = 18$ mm. The design of other slot configurations was also guided by this optimization-based approach.

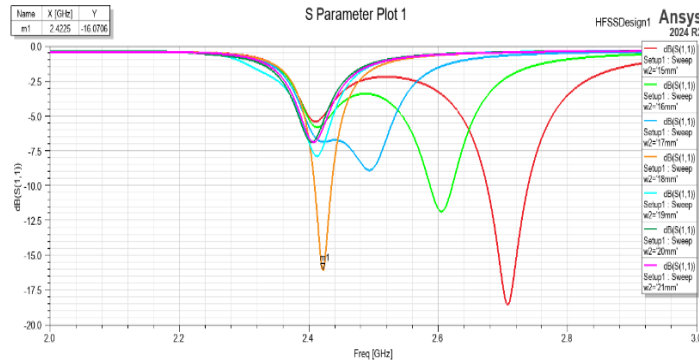


Fig.4. S_{11} results were obtained through an iterative method applied to the parameter w_2 .

The primary objective of this design is to effectively control the distribution of electric and magnetic fields on the antenna surface, thereby improving radiation characteristics. As illustrated in Figure 5(a), the surface current density which is essential for antenna efficiency and effective signal propagation primarily flows through the feed line and the lower part of the patch, reaching a peak value of approximately 963 A/m. This current distribution highlights the key radiating regions that contribute to the main radiation patterns and plays a significant role in the reduction of f_r . Furthermore, in Figure 5(b), the maximum electric field strength of the antenna is measured at 84.890 V/m. The increase in electric field intensity in specific regions (highlighted in red and yellow) indicates that the antenna is radiating more strongly in certain directions. These findings confirm that the surface current density variations are sufficiently high to facilitate efficient radiation, with the primary radiation occurring in these high-field regions.

The comparison of S_{11} values obtained in the simulation environment, based on the optimization processes applied during the antenna design stages, is presented in Figure 6. In Figure 6 four curves (a-d) correspond to different antenna configurations: (a) the conventional antenna (2.15 GHz), (b) the antenna with both stub and slot (2.45 GHz), (c) the antenna without a stub but with a slot (2 GHz), and (d) the antenna with a stub but without a slot (2.22 GHz). The results indicate that when both stub and slot modifications are implemented simultaneously, the f_r of the proposed antenna is observed at 2.45 GHz, with an S_{11} value of -15.76 dB at this frequency. Furthermore, the antenna does not achieve the desired performance solely through either stub or slot modifications. The results suggest that neither of these individual adjustments is sufficient to ensure proper operation at the intended frequency. Similarly, the conventional antenna design, without these optimizations, fails to achieve the required impedance matching and does not meet the performance criteria for efficient radiation.

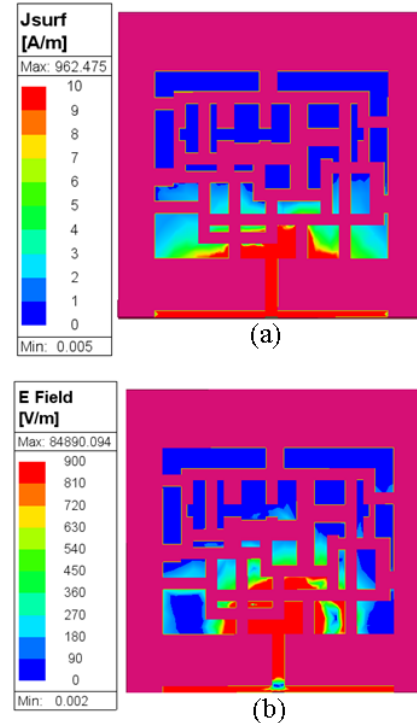


Fig. 5. Simulation results of the proposed antenna, (a) Surface current and (b) Electric field distributions.

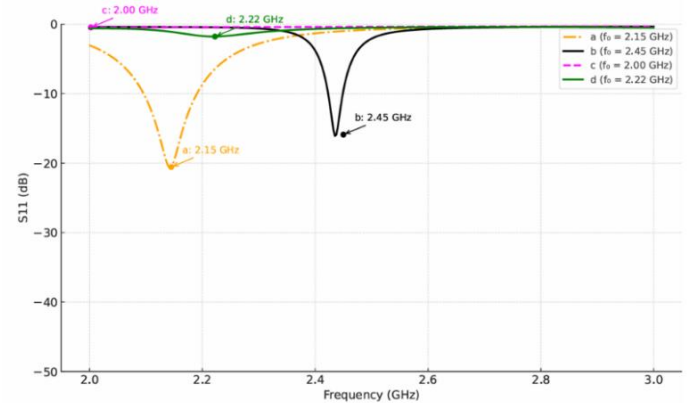


Fig. 6. Return Loss (S_{11}) simulation results for rectangular patch antenna geometries.

A comparison between the S_{11} measurements and the simulation results is provided in Figure 7. The measurement and simulation results are in close agreement, indicating excellent impedance matching and minimal power reflection.

Minor discrepancies between simulated and measured results are commonly observed in practical implementations due to fabrication imperfections and connector-induced parasitic effects. According to IEEE antenna standards, an antenna is considered to operate efficiently when the S_{11} is below -10 dB, indicating acceptable impedance matching and minimal power reflection. Therefore, the proposed antenna maintains $S_{11} < -10$ dB within the target operational range, ensuring efficient power transfer and reliable operation at 2.45 GHz.

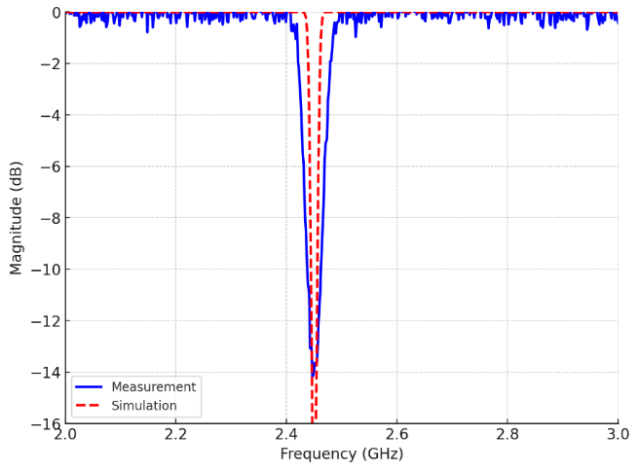


Fig. 7. Measurement and simulation comparison of S_{11} parameter.

The radiation patterns of the conventional antenna and the proposed antenna, as depicted in Figure 8, indicate that the maximum radiated power occurs at $\theta = 0^\circ$. However, the measured radiation pattern of the conventional antenna in Figure 8(a) shows a half-power beamwidth (HPBW) of 102.5° , whereas the proposed antenna design in Figure 8(b) achieves a narrower HPBW of 90° , indicating improved directivity.

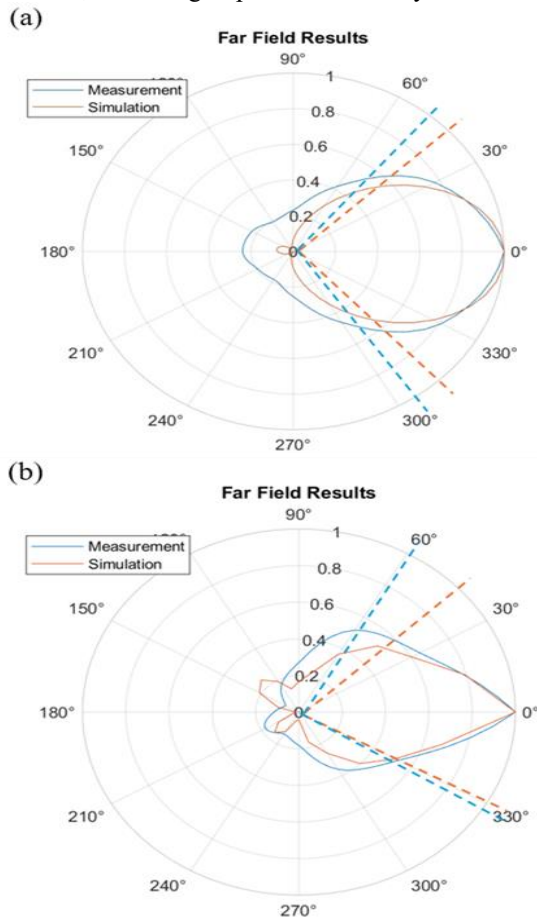


Fig. 8. Comparison of normalized (at $\phi=0^\circ$) radiation patterns (E-plane) of measured and simulated antennas; (a) the conventional rectangular patch and (b) proposed antennas.

Figure 9 presents the 3D radiation pattern and gains a comparison of the conventional and proposed patch antenna. In both cases, the maximum radiated power is observed at $\theta = 0^\circ$, confirming a broadside radiation characteristic, which is typical for patch antennas. The colour gradient represents the relative intensity of the radiated power, where red regions indicate high-intensity radiation and blue/green areas correspond to lower intensity levels. Consequently, modifying the conventional patch antenna into the proposed structure has resulted in approximately a 148% increase in antenna gain, indicating a significant improvement in directivity and overall performance.

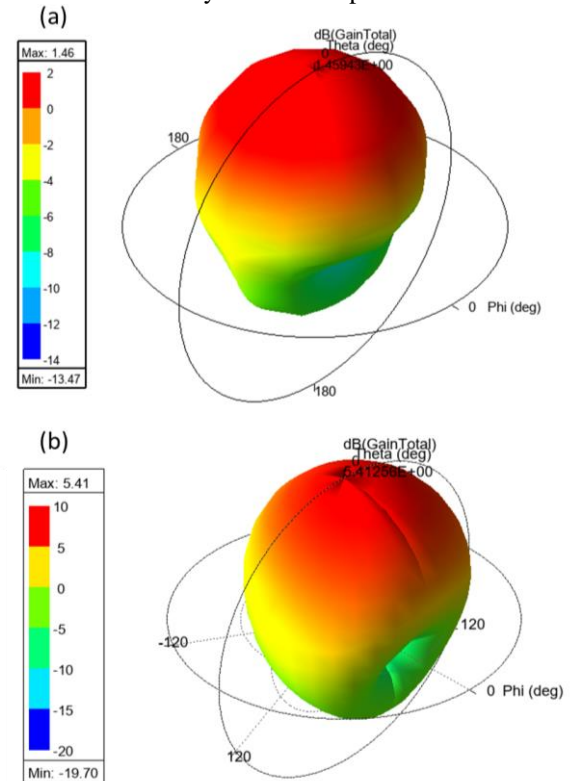


Fig. 9. 3D radiation pattern and antenna gains of (a) Conventional and (b) Proposed patch antennas.

In MPA design, various techniques and optimizations are employed to enhance performance for specific applications. Table 2 provides a comparative analysis of various antenna designs based on physical dimensions, operating frequency, and gain. Among the studies listed in Table 2, [14] and [18] focus on dual-band designs intended for RFID and WLAN applications, respectively. In [15] present a triple-band design aimed at GPS, DCS, WLAN, and WiMAX applications. In [16] improvements in cross-polarization characteristics, while in [17] emphasize compact antennas with circular polarization properties. Each design has been specifically optimized to meet the requirements of its respective application, offering distinct advantages based on the targeted use case. The antenna proposed in this study features a compact size of $50 \times 50 \text{ mm}^2$, operating at 2.45 GHz with a gain of 5.41 dBi. Compared to other designs, it delivers a higher gain despite its smaller footprint, indicating more efficient radiation and improved directivity. Therefore, the proposed antenna offers an optimal balance between compact size and high-gain

performance. Notably, when comparing this design to the antenna presented in [14], which operates at 2.4 GHz with a gain of 2.36 dBi and dimensions of $60 \times 70 \text{ mm}^2$, the proposed antenna can be considered both more compact and higher in gain.

Table 2. Comparison of the designed antenna with some antennas from the literature.

Antenna Size (mm^2)	Frequency (GHz)	Gain (dBi)	References
60×70	2.4 and 5.8	2.36	[14]
110×68	1.8 and 2.4	3.02	[15]
70×70	2.53	3.84	[16]
100×100	1.039-1.094	2.5	[17]
50×50	2.4 and 5.8	1.17	[18]
40x23	2.43	1.73	[19]
50×50	2.45	5.41	This study

4. CONCLUSION

The MPA designed in this study, intended for Wi-Fi (2.4 GHz band) and Bluetooth applications, operates at a resonant frequency (f_r) of 2.45 GHz. The S_{11} parameters of this antenna, with dimensions of $50 \times 50 \text{ mm}^2$ and a microstrip feed, were analyzed and compared to the original patch antenna. Optimization techniques, including slotting in the patch and stub modifications in the feed, were employed to enhance performance. The analysis of the electric field and surface current distributions revealed that the feeding line exhibited the highest radiation. The measured radiation pattern confirmed that the main beam, with the highest directivity, is oriented at $\theta = 0^\circ$, aligning with the expected broadside radiation characteristic. The reflection coefficient is ideally expected to be smaller than -10 dB in IEEE standards and was measured at -14.4 dB. Additionally, the maximum gain of the proposed antenna was calculated as 5.41 dBi, which is considered a strong performance for Wi-Fi and Bluetooth applications.

Acknowledgement

The authors would like to thank for the contributions of Recep Tayyip Erdoğan University Electromagnetic Application and Research Center (REMAM).

References

- [1] A. Öncü, K. Özenç, and M. E. Aydemir, "Design of a dual-layer high-gain rectangular microstrip patch antenna operating at 1.26 GHz resonance frequency," *Gazi University Journal of Engineering and Architecture Faculty*, 28(4), pp. 743–750, 2013.
- [2] P. Bhartia, I. Bahl, R. Garg, and A. Ittipiboon, *Microstrip Antenna Design Handbook*. Boston, MA: Artech House Publishers, 2000.
- [3] O. Gürdoğan, A. E. Aydın, and S. C. Başaran, "Multilayered implantable antenna design for biotelemetry communication," *Turkish Journal of Electromechanics and Energy*, 3(1), pp.27-30, 2018.
- [4] M. I. Nawaz, Z. Huiling, M. S. Sultan Nawaz, K. Zakim, S. Zamin, and A. Khan, "A review on wideband microstrip patch antenna design techniques," in *Proceedings of the 2013 International Conference on Aerospace Science & Engineering (ICASE)*, Islamabad, Pakistan, August 2013, pp. 1–8.
- [5] S. N. Ather and P. Singhal, "Truncated rectangular microstrip antenna with H and U slot for broadband," *International Journal of Engineering Science and Technology*, 5(1), pp. 114-118, 2013.
- [6] C. D. Erbaş, "Dual-band and dual-mode slotted ring microstrip patch antenna for GSM-1800 and GPS applications," *Gazi University Journal of Engineering and Architecture Faculty*, 38(1), pp. 547–556, 2022.
- [7] S. Chen, D. Dong, Z. Liao, Q. Cai, and G. Liu, "Compact wideband and dual-band antenna for TD-LTE and WLAN applications," *Electronics Letters*, 50(16), pp. 1111–1112, 2014.
- [8] S. Sharma, C. C. Tan, and R. Rishi, "Impedance matching techniques for microstrip patch antenna," *Indian Journal of Science and Technology*, 10(28), pp. 1–16, 2017.
- [9] D. M. Pozar, *Microwave Engineering*, 4th ed. Hoboken, NJ: John Wiley & Sons, 2011.
- [10] H. Arai, G. J. Durnan, and S. Saito, "A dual element patch array antenna structure with microstrip triple stub matching," in *Proceedings of the IEEE Antennas and Propagation Society International Symposium*, Columbus, USA, Jun. 2003, vol. 4, pp. 528–531.
- [11] H. Chen and S.-Y. Chen, "A polarization-agile stub-loaded square patch antenna with proximity coupled feed," in *Proceedings of the 2018 IEEE International Symposium on Antennas and Propagation and USNC/URSI National Radio Science Meeting*, Boston, USA, Jul. 2018, pp. 859–860.
- [12] M. P. Mohan, L. Zhao, J. Jimeno, A. Alphones, M. Y. Siyal, and M. F. Karim, "Design of stub loaded transmission line matching circuit for series fed patch array," in *Proceedings of the 2021 IEEE International Symposium on Antennas and Propagation and USNC-URSI Radio Science Meeting*, Marina Bay Sands, Singapore, Dec. 2021, pp. 1279–1280.
- [13] Y. Karan, and N. As, "Electromagnetic radiation measurement of a high gain wireless network adapter," *Turkish Journal of Electromechanics and Energy*, 1(2). pp. 17-23, 2016.
- [14] R. Karli and H. Ammor, "Rectangular patch antenna for dual-band RFID and WLAN applications," *Wireless Personal Communications*, 83(2), pp. 995–1007, 2015.
- [15] J. Park, M. Jeong, N. Hussain, S. Rhee, P. Kim, and N. Kim, "Design and fabrication of triple-band folded dipole antenna for GPS/DCS/WLAN/WiMAX applications," *Microwave and Optical Technology Letters*, 61(5), pp. 1328–1332, 2019.
- [16] J. Kaur, Nitika, and R. Panwar, "Design and optimization of a dual-band slotted microstrip patch antenna using Differential Evolution Algorithm with improved cross polarization characteristics for wireless applications," *Journal of Electromagnetic Waves and Applications*, 33(11), pp. 1427–1442, 2019.

[17] X. L. Bao and M. J. Ammann. "Compact annular-ring embedded circular patch antenna with cross-slot ground plane for circular polarisation," *Electronics Letters*, 42(4), pp. 192–193, 2006.

[18] S. Küçükcan and A. Kaya, "Dual-band microstrip patch antenna design for Wi-Fi applications," *European Journal of Science and Technology*, Spec. 34, pp. 661–664, March 2022.

[19] J. Islam, M. Rahman, and A. Z. M. Touhidul Islam, "Design of a polyester substrate based microstrip patch antenna for WBAN applications," *International Journal of Recent Engineering Science*, 10(3) pp. 77–83, 2023.

Biographies



Mehmet Durmuş Çalışır completed his undergraduate studies in Materials Science and Engineering and Electronics Engineering at Gebze Technical University in 2012, his master's degree at Istanbul Technical University in 2014, and his PhD in Nanoscience and Nanoengineering in 2020, focusing on the production and applications of nano-structured metal oxide materials. He currently works as an Assistant Professor at Recep Tayyip Erdoğan University and has research interests in nanofiber technologies, energy and environmental applications, and IoT systems.

E-mail: mehmetdurmus.calisir@erdogan.edu.tr



Hilal Sena Altaş received her B.Sc. degree in Electrical and Electronics Engineering from Recep Tayyip Erdoğan University, Rize, Türkiye, in 2024, graduating as the top student in her department. During her undergraduate studies, she focused on RF systems, EMC design, antennas, and radar-absorbing materials. She completed internships at Baykar Technologies in EMC engineering and Aydın Textile in maintenance and integration systems. Her main research interests include antenna design, RF/microwave systems, EMC/EMI analysis, and radar cross-section reduction techniques.

E-mail: hilalsena_altas20@erdogan.edu.tr



Caner Murat is currently affiliated with the Department of Electrical and Electronics Engineering at Recep Tayyip Erdoğan University. His research interests include microwave circuits, electromagnetic applications in medicine, and antenna design. He received his B.Sc. degree from İzmir Katip Çelebi University in 2017, followed by an M.Sc. degree in 2019 and a PhD in 2023, focusing on microwave ablation systems for cancer treatment. He completed his postdoctoral research at the Karlsruhe Institute of Technology (KIT), Germany, where he investigated advanced microwave material processing techniques.

E-mail: caner.murat@erdogan.edu.tr